*energies*

Formatted: Numbering: Continuous

*Article*

# Experimental study regarding radiation noise characteristic of centrifugal pump with various working conditions

**Chang Guo [1], Ming Gao [2,*], Dongyue Lu [3] and Kun Wang [4]**

[1] School of Energy and Power Engineering, Shandong University, Jinan 250061, China; gg3263@163.com
[2] School of Energy and Power Engineering, Shandong University, Jinan 250061, China; gm@sdu.edu.cn
[3] State Nuclear Power Engineering Company, Shanghai 200233, China; ldy11energy@163.com
[4] School of Energy and Power Engineering, Shandong University, Jinan 250061, China; sduwang1993@163.com

* Correspondence: gm@sdu.edu.cn; Tel.: +86-~~159-6663-8936~~88399008

**Abstract:** Aiming at investigating the radiation noise characteristic of centrifugal pump under various working conditions, a noise measurement system is established, afterwards, the distribution of different points and intervals, as well as the overall level of noise are studied. The total sound pressure level distribution for different points manifests the dipole and asymmetric directivity characteristic. Additionally, the acoustic energy is introduced to compare the noise of different intervals to reveal the asymmetric characteristic, it is found that the variation of working condition has ~~slight~~little impact on the acoustic energy distribution, and the ratio of the acoustic energy in the direction facing the tongue, as well as that in the direction against the tongue to total acoustic energy ~~fluctuates~~fluctuate around 0.410 and 0.160, respectively, under various working conditions. Besides, the A-weighted average sound pressure level ($L_{pA}$) is applied to describe the overall level of noise, and $L_{pA}$ increases gradually with the growth of rotational speed, but the growth slope decreases. While in the operation of throttling regulation, $L_{pA}$ shows the trend that increases firstly, then maintains stably, and increases again with the growth of flow rate. This study could provide guidance for optimizing the operating conditions and noise control of centrifugal pumps.

**Keywords:** centrifugal pump; radiation noise; distribution characteristic; acoustic energy; experimental research

## 1. Introduction

~~With~~ Widespread concerns on the ~~development of technology and improvement of people's awareness of~~ environmental protection~~, noise hazard has increasingly drawn widespread attention, and~~ accelerate the noise abatement investment~~ has accounted~~, accounting for 15%-20% of the environmental protection investment [1]. The centrifugal pumps, ~~as are~~ widely applied in many fields of national economy [2,3], radiate a lot of noise during operation~~, which~~. The unexpected noise could affect the flow performance and deteriorate the working environment~~, and has become a major pollution hazard. Actually, the working condition of centrifugal pumps always changes to meet different working demands, which could cause the radiation noise also changes with the working condition.~~. To establish theoretical basis ~~for~~of the radiation noise control technology ~~of~~for centrifugal pumps, this study reveals the changing rules of radiation noise under various working conditions.

~~For research on noise of centrifugal pumps, experimental study provides~~Experimental studies could provide the most reliable results~~, which has been widely adopted by~~ for scholars~~.~~ to detect the noise from centrifugal pumps. Choi et al. [4] conducted experiment and revealed that the main cause of radiation noise generated by impeller without volute was the pressure fluctuation on blade surface ~~induced by flow field instability in~~. Chu et al. [5,6] took the ~~impeller, while~~volute into consideration and attributed the primary ~~source of~~ noise ~~in centrifugal pumps including a volute is associated~~

~~with~~to the interaction between the non-uniform outflux from impeller and tongue [5,6], and the further research showed that a slight increase of the gap between impeller and tongue would reduce the noise ~~level~~ significantly [7]. Parrondo et al. [8] established an acoustic model to characterize the internal sound field at low frequency range, and concluded that the internal sound field could be characterized by a dipole-like source ~~located~~ near the tongue. Cai et al. [9] measured the pressure fluctuation near the wall of tongue under various rotational speed conditions, and found that the pressure fluctuation intensity ~~of pressure fluctuations near the tongue~~ increased more rapidly than ~~the increase~~that of rotational speed. ~~To further study the characteristic of internal sound field in pipe, four~~Four-port model was introduced for the ~~correlational~~ research~~, which provided~~ of internal sound field in pipe, providing the convenience for the ~~study about the~~ changing rules of noise in ~~inlet and outlet~~ pipe under various ~~medium temperature [10], rotational speed and flow rate~~working conditions [~~11,~~10-12]. Based on LabVIEW, Yuan et al. [13] designed a measurement system for internal noise analysis of centrifugal pumps~~, which realized the~~ with synchronous measurement ~~of~~for noise signal~~ in pipe~~, pressure and flow rate, and laid a foundation for the follow-up study about the influence of different ~~centrifugal pumps structure~~structures [14-16] on ~~internal~~ sound ~~field under various flow rate conditions~~pressure level (SPL) at different frequencies. To characterize the feature of far field radiation noise, Ye et al. [17] measured the noise amplitude outside a centrifugal pump under various flow rate conditions~~ on account of near field acoustic pressure method~~, and ~~it was~~ found that noise amplitude~~ increased with the flow rate and~~ reached maximum at the highest efficiency point.

Currently, ~~numerical simulation has become~~as a useful research tool, ~~which provided complementary with~~numerical simulation compensated shortages for experiment. ~~As the study progressed, a~~A hybrid method combining computational fluid dynamics (CFD) with Lighthill acoustic analogy was widely used to elucidate the acoustic generation [18,19]. Langthjem et al. [20,21] applied the hybrid method for noise calculation in a two-dimensional centrifugal pump, and concluded that the main cause of noise ~~is~~was the dipole source. The dipole source was defined as unsteady fluid force acting on the wall surface~~, which mainly included~~ including impeller ~~dipole source~~ and volute ~~dipole~~ source in centrifugal pumps. Huang et al. [22], Ma et al. [23] and Liu et al. [24] ~~took~~considered the two ~~different~~ dipole sources as the noise source for acoustic calculation ~~separately~~, and compared the ~~sound pressure level (~~SPL~~) of radiation noise~~ at different ~~order~~orders of blade passing frequency (BPF) with different structures, ~~which could provide~~and these researches provided guidance for structural optimization of centrifugal pumps. In addition, Gao et al. [25] ~~analyzed the directivity characteristic of radiation noise generated by the two different dipole sources separately, it was~~ discovered that the radiation noise generated by impeller demonstrated the diploe directivity characteristic, while the volute-generated noise appeared an apparent asymmetric directivity characteristic~~ that~~, i.e., the noise level in the direction facing the tongue was higher than that of the direction against the tongue~~, and~~. Dong et al. [26] ~~explored the relationship between radiation noise~~ pointed out that the volute-generated ~~by volute dipole source and rotational speed, the volute generated noise showed the trend that~~ noise increased monotonously and nonlinearly with the increase ~~in rotating~~of rotational speed.

Obviously, ~~according to the above~~ literature ~~review,~~goes that previous experimental research mainly focused on the internal noise characteristic in pipe, however, ~~less~~merely experimental research ~~has been carried out~~focused on the far field radiation noise. During the numerical simulation, the previous research mainly considered the influence of impeller dipole source and volute dipole source on the radiation noise separately, and ~~the~~ most ~~study objects~~ are the SPL at different ~~order~~orders of BPF~~, while the TSPL characteristic is ignored.~~. Actually, ~~during the operation of centrifugal pumps,~~ the radiation noise ~~is~~results from the interaction ~~result~~ of the two dipole source when pumps are running, so the interaction influence should be considered to obtain more accurate results. ~~As a result of the directionality in~~In addition, it is necessary to calculate the total sound ~~propagation, different space points with respect to sound source have different directions, which results in noise directional difference of different points, on another side, the radiation noise~~pressure level (TSPL) of different monitoring points~~ is~~, calculated by the superposition ~~results~~ of SPL at different characteristic frequencies, ~~it is necessary to calculate the TSPL of different monitoring points to acquire the directivity characteristic. Furthermore, because noise~~Noise propagation is the ~~propagation~~spread of acoustic energy in the medium, thus, the acoustic energy ~~will change in the~~changes with noise propagation process ~~of noise propagation as the distance from the sound source changes, so it is also considered to describe~~and the directivity characteristic~~.~~ can be detected. Besides, the overall level of radiation noise should be conducted to evaluate the noise ~~level~~intensity under ~~a certain~~specific working ~~condition. What's more, centrifugal~~ conditions. In general, the pumps ~~need to work~~ are always working at various conditions ~~to meet~~with various working demands, ~~which could cause~~and the radiation noise ~~changing inevitably~~changes accordingly, it is also indispensable to carry out the various working condition study for radiation noise to figure out the changing rules.

~~Therefore~~In this paper, a centrifugal pump radiation noise measurement system is established ~~in this paper. In the system, the centrifugal pump and motor are insulated by a soundproof room to reduce the influence of surrounding environment and motor operation on measurement results,~~. And then the TSPL and acoustic energy distribution characteristic ~~on measurement surface in circumferential direction~~, as well as overall level characteristic of radiation noise are analyzed ~~under various working conditions to reveal the changing rules of radiation noise~~, which may provide guidance for optimizing the working conditions and noise control of centrifugal pumps.

## 2. Experimental facility and procedure

### *2.1. Parameters of the test pump*

In this study, IS-80-50-250 is chosen as the test pump, and the prototype figure is shown in Figure 1. Water at normal temperature is used as medium, and the geometric and performance parameters of the test pump are listed in Table 1.

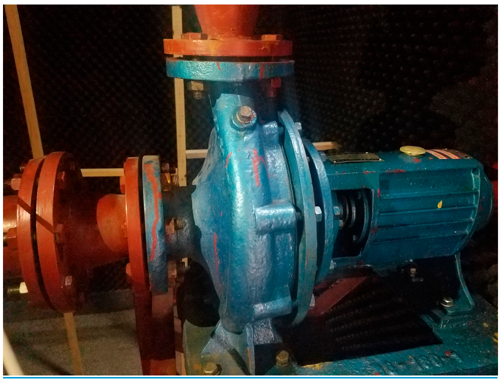

**Figure 1.** Prototype figure of the test pump

**Table 1.** Geometric and performance parameters of the test pump.

| Parameter | Value |
|---|---|
| Inlet diameter , mm | 80 |
| Impeller diameter , mm | 250 |
| Outlet diameter, mm | 50 |
| Nominal flow rate, $m^3$/h | 50 |
| Best efficiency | 63% (50 $m^3$/h) |
| Design head, m | 80 |

**Formatted:** Line spacing: At least 13 pt
**Formatted:** Line spacing: At least 13 pt
**Formatted:** Line spacing: At least 13 pt
**Formatted:** Line spacing: At least 13 pt
**Formatted:** Line spacing: At least 13 pt
**Formatted:** Line spacing: At least 13 pt

| | |
|---|---|
| Nominal ~~rotating~~rotational speed, rpm | 2900 |
| Blade number | 6 |

Formatted: Line spacing: At least 13 pt

Formatted: Line spacing: At least 13 pt

### *2.2. Radiation noise measurement system*

The experimental apparatuses used in the system are shown schematically in Figure ~~1~~2, which ~~includes~~include soundproof room, water circulation system, circuit control system, data acquisition and storage system. In the measurement system, to reduce the influence of surrounding environment and motor operation on the measurement results, the centrifugal pump and motor are insulated by a soundproof room, the interior and exterior walls of soundproof room, along with the motor are surrounded by soundproof cotton~~ to reduce the influence of surrounding environment and motor operation on the measurement results of radiation noise.~~. Besides, the pump is driven by the YVF2180L-2 type three-phase asynchronous motor, and the rotational speed is regulated by Y0300G3 type frequency converter. The flow rate, inlet pressure, outlet pressure, as well as the radiation noise level are measured and recorded by corresponding instrument listed in Table.2.

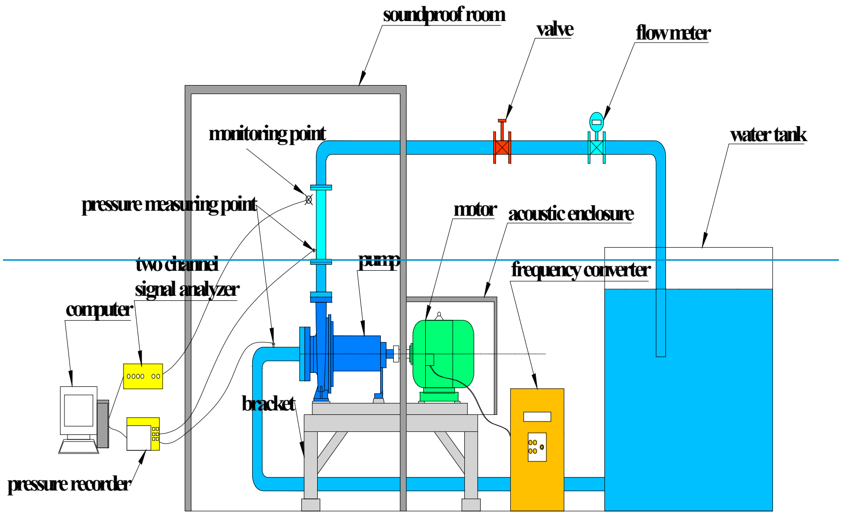


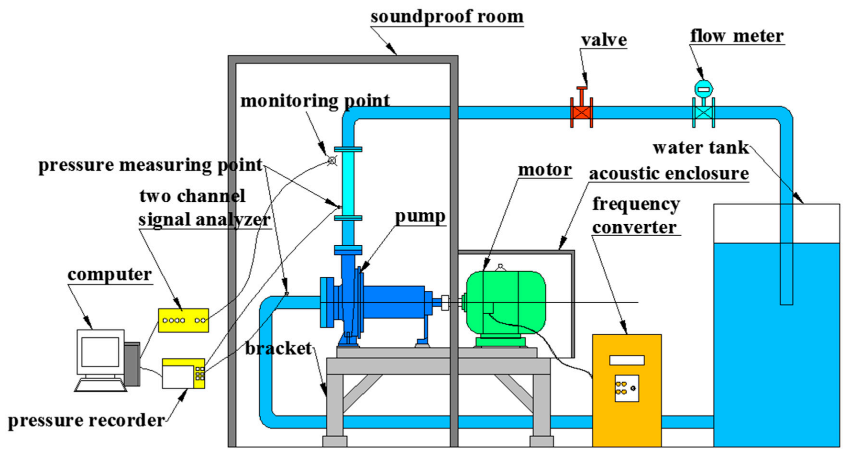


**Figure ~~1~~2**. Layout and instrumentation of measurement system

Formatted: Indent: First line: 0 cm

**Table 2.** Measurement characteristic of instruments

| Instruments | Type | Application | Measuring range | Accuracy or sensitivity |
|---|---|---|---|---|
| Flow meter | SLDG-800 | Measuring flow rate | 0-100m³/h | 0.2% (accuracy) |
| Pressure transducer | MIK-300 | Measuring inlet pressure | -100-0kPa (inlet pipe) | 0.5% (accuracy) |
| | | Measuring outlet pressure | 0-1600kPa (outlet pipe) | 0.5% (accuracy) |
| Pressure recorder | RX-200D | Recording pressure | / | / |
| Microphone | AWA14423L | Measuring radiation noise | 10-20kHz | 50mV/Pa (sensitivity) |
| Two channel signal analyzer | AWA6290M+ | Recording radiation noise | / | / |

During the operation, when the operation system reaches stable, the flow rate, pressure, radiation noise level are measured sequentially and stored in computer terminal ~~when the operation system is stable, after~~. After that, the rotational speed ~~or~~and flow rate are adjusted via frequency converter and artificial regulation, respectively, then these parameters under various working conditions are recorded for analysis. Figure ~~2~~3 shows the structure diagram of measurement system.

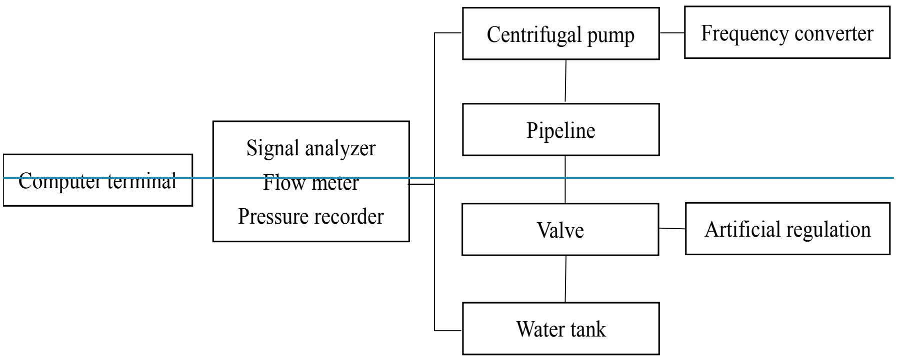


**Formatted:** Line spacing: At least 13 pt
**Formatted:** Line spacing: At least 13 pt
**Formatted:** Line spacing: At least 13 pt
**Formatted:** Line spacing: At least 13 pt
**Formatted:** Line spacing: At least 13 pt
**Formatted:** Line spacing: At least 13 pt

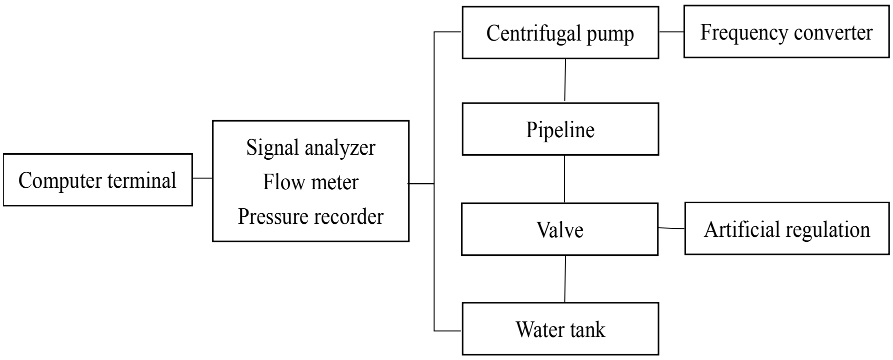


**Figure ~~2~~3.** Structure diagram of measurement system

## 2.3. *Arrangement of the monitoring points*

To acquire the distribution characteristic of radiation noise, 16 monitoring points are arranged on the measurement surface around the pump~~, as~~. As shown in Figure ~~3~~4, the monitoring points are 1000mm away from the center of impeller, ~~which~~and arranged evenly in~~ the~~ circumferential direction [27]. During the measurement process, SPL characteristic of every point is measured by microphone sequentially. Here, SPL is defined as,

$$SPL = 20log\frac{P_e}{P_{ref}} \tag{1}$$

$$P_e = \sqrt{\frac{1}{T}\int_0^T p'^2 dt} \tag{2}$$

$$T = \frac{t}{l} \tag{3}$$

where $P_{ref}$ is the reference acoustic pressure ($2*10^{-5}$Pa in air), ~~while~~ $P_e$ is the effective value of acoustic pressure~~ defined as~~, $p'$ is instantaneous acoustic pressure, $t$ is the time of one revolution of impeller, and $l$ is the number of blades ($l$=6 in this paper).

$$\cancel{P_e = \sqrt{\frac{1}{T}\int_0^T p^2 dt}} \tag{2}$$

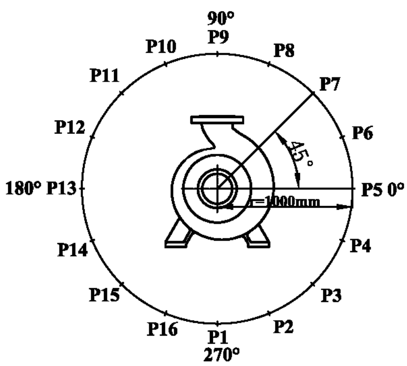

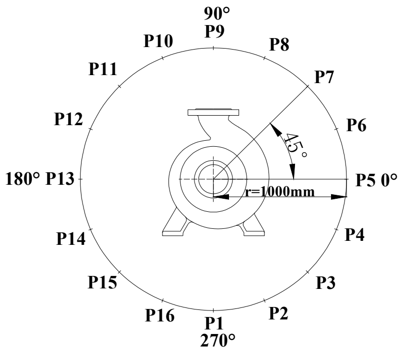


**Figure ~~3~~4.** Arrangement of monitoring points in circumferential direction

To ~~figure out~~reveal the~~ radiation~~ noise intensity of different monitoring points and the directivity characteristic~~ of radiation noise~~, it is necessary to derive a temporal intensity profile involving a superposition of ~~acoustic pressures~~SPL at each Fourier frequency~~, so~~. Thus TSPL is introduced ~~in this paper~~ and given by,

$$\cancel{TPSL = 10\,lg\sum_{i=1}^{n} 10^{SPL_i/10}} \qquad \cancel{(3)}$$

$$TPSL = 10\,lg\sum_{i=1}^{n} 10^{SPL_i/10} \qquad (4)$$

where $n$ represents the number of frequencies. However, TSPL only represents the noise level of a certain monitoring point, and it can't be superimposed by arithmetic to describe the noise level of an interval. Therefore, the acoustic energy is more suitable for comparing the noise level of different monitoring intervals since it can be superimposed by arithmetic, moreover, the propagation of sound is essentially the propagation of energy. Briefly, the application of acoustic energy could reveal the noise level relationship between different intervals intuitively, so the average acoustic energy density [28] is analyzed, ~~which~~and it is defined as,

$$\varepsilon = \frac{P_e^2}{\rho c^2} \qquad (\cancel{4}5)$$

where $\mathcal{E}$, $\rho$ and $c$ ~~represents~~represent the acoustic energy density, medium density (1.29kg/m$^3$ in air) and the sound speed in medium (343m/s in air), respectively.

To further evaluate the overall level characteristic of radiation noise on measurement surface, the average A-weighted sound pressure level ($L_{pA}$) of the measurement surface is introduced and expressed as,

$$L_{pA} = 10\,lg(\frac{1}{m}\sum_{i=1}^{m} 10^{TSPL_i/10}) \qquad (\cancel{5}6)$$

where $m$ represents the number of monitoring points, and the $L_{pA}$ of 16 monitoring points on the measurement surface around the pump is calculated for analysis.

## 3. Radiation noise characteristic under various rotational speed conditions

~~In the operation of~~The variable speed regulation~~, the pump performance characteristic curve is adjusted by regulating the speed, this method~~ has no throttling loss, ~~which makes it~~and is an ideal adjustment method. In this section, on the basis of keeping the flow valve installed downstream on the outlet pipe opened fully and unchanged, ~~which ensures~~then the ~~pipeline~~radiation noise characteristic ~~unchanged, then the pump duty point is regulated by frequency converter~~under various rotational speed conditions are studied. According to the similarity law, the relationship between flow rate and rotational speed is defined as,

$$\frac{Q_1}{Q_2} = \frac{n_1}{n_2} \quad \text{~~(6)~~}$$

$$\frac{Q_1}{Q_2} = \frac{n_1}{n_2} \quad (7)$$

where $Q$ and $n$ ~~represents~~represent the flow rate and rotational speed, while the subscript 1 and 2 ~~represents~~represent two different working conditions~~, respectively~~. It can be found that the flow rate is proportional to the rotational speed, so the flow rate of centrifugal pump is increasing with the ~~increase~~rise of rotational speed. To ensure the safety of the running system, seven different rotational speeds that are less than or equal to the ~~rated~~nominal rotational speed~~, including 1700, 1900, 2100, 2300, 2500, 2700, 2900rpm,~~ are ~~measured to reveal the radiation noise changing rules under various~~considered. The rotational ~~speed conditions~~speeds and corresponding flow rates are shown in Table 3.

**Table 3**. Rotational speeds and corresponding flow rates

| Rotational speed, rpm | Flow rate, m³/h |
|---|---|
| 1700 | 56.9 |
| 1900 | 64.8 |
| 2100 | 69.6 |
| 2300 | 74 |
| 2500 | 78.2 |
| 2700 | 82.1 |
| 2900 | 86 |

*3.1. Directivity characteristic of radiation noise under various rotational speed conditions*

By measuring the SPL characteristic and calculating the ~~TSPL~~TSPLs of 16 different points in the circumferential direction, the directivity characteristic of radiation noise is ~~studied~~obtained under various rotational speed conditions.

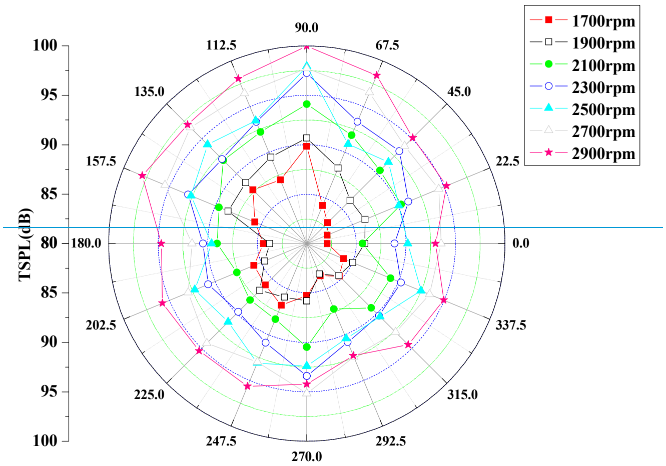

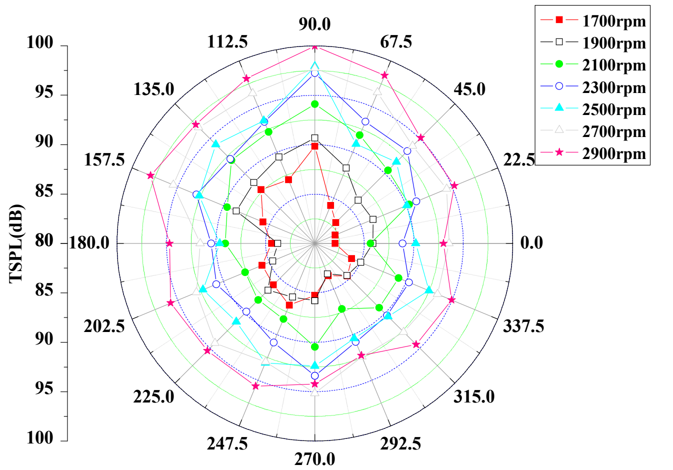


**Figure ~~4~~5.** Directivity characteristic of radiation noise under various rotational speed conditions

Formatted: Centered, Indent: First line: 0 cm

As shown in Figure ~~4~~5, it can be found that the TSPL increases ~~in the range of~~from 80 to 100dB with the increase of rotational speed. As a result of the symmetric characteristic of impeller, the ~~profiles~~profile of directivity diagram of TSPL ~~demonstrate~~demonstrates the dipole symmetric characteristic, ~~it is also found~~and one sees that the two TSPL valleys appear at 0° and 180°. In addition, apparent asymmetric characteristic also can be found due to the asymmetric structure of volute, more concretely, the noise level in the direction facing the tongue (in the interval from 90° to 157.5°) is higher than that in the direction against the tongue (in the interval from 292.5° to 0°), which means that the radiation noise is the interaction result of ~~a combination of~~ impeller and volute dipole source.

To further reveal the asymmetric characteristic under various rotational speed conditions quantitatively, the ratio of the acoustic energy in the interval from 90° to 157.5° ($\varepsilon_1$), as well as that in the interval from 292.5° to 0° ($\varepsilon_2$) to the total acoustic energy ($\varepsilon_t$) are calculated. As shown in Figure ~~5~~6, the ~~value~~values of $\varepsilon_1/\varepsilon_t$ and $\varepsilon_2/\varepsilon_t$ ~~have~~change little ~~change~~ with the ~~increase~~change of rotational speed, and the value of $\varepsilon_1/\varepsilon_t$ fluctuates around 0.413, while the value of $\varepsilon_2/\varepsilon_t$ fluctuates near 0.157~~, which means~~. It proves that the change of rotational speed would affect the acoustic energy, but it has ~~slight~~little impact on the acoustic energy distribution. ~~On the one hand, according~~According to the ~~previous researches~~past research [5-7], the volute tongue is the ~~key~~major noise source, and the measurement interval in the direction facing the tongue is ~~more~~ closer to the tongue than other intervals~~, on~~. On the other hand, acoustic energy ~~attenuates~~weakens gradually as the distance from the sound source increases, so the acoustic energy has ~~slight~~less attenuation in the direction facing the tongue~~, and causes the~~ than that in the direction against the tongue, causing a much higher ratio of acoustic energy in the direction facing ~~the tongue much higher than that in the direction against~~ the tongue.

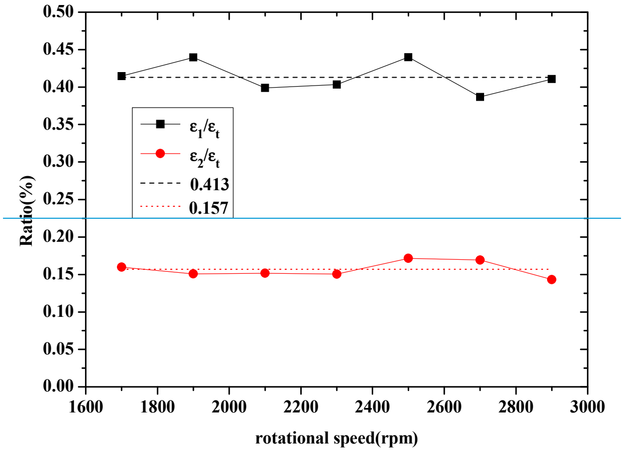


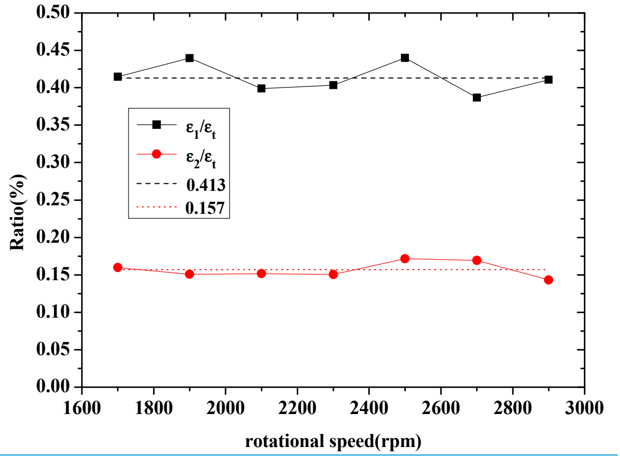


**Figure ~~5~~6.** The acoustic energy changing curves with rotational speed

*3.2. Changing rules of radiation noise under various rotational speed conditions*

~~The~~To analyze the noise level changing rules of different points under various rotational speed conditions, P1 (270°, in the direction against the outlet), P5 (0°, the valley point), P9 (90°, in the direction facing the outlet), P11 (135°, in the direction facing the tongue) and P13 (180°, the valley point) are selected~~ to analyze the changing rules of noise level under various rotational speed conditions.~~. As shown in Figure ~~6~~7, it can be more visually ~~see~~seen that the ~~TSPL rising trend~~TSPLs of different monitoring points ~~along~~rise with the rotational speed increasing. In general, ~~TSPL~~TSPLs of P5 and P13 are lower than others because the two points are located at the valley of dipole characteristic, meanwhile, TSPL of P1 lies between P5 and P11~~, moreover, as~~. As a result of the influence of volute tongue noise source, P9 and P11 have a higher noise level, and P9 is located in outlet direction, which is more affected by the internal flow noise in outlet pipe, so P9 is the highest noise level point.

**Formatted:** Space After: 0 pt

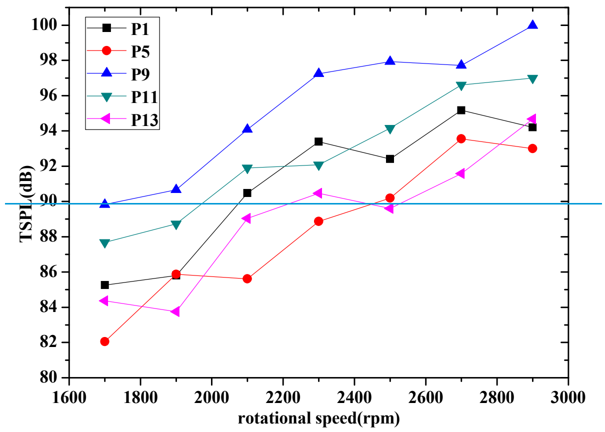


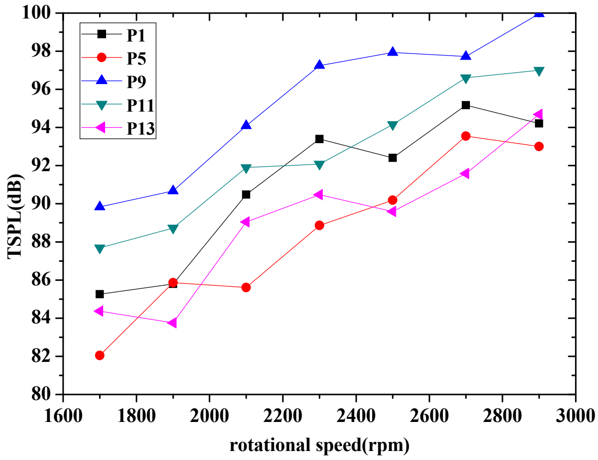


**Figure ~~6~~7.** TSPL changing curves with rotational speed

To evaluate the overall level of radiation noise, the $L_{pA}$ of the 16 monitoring points is compared in Figure ~~7.~~8 under various rotational speed conditions. It can be observed that $L_{pA}$ ~~increases~~climbs gradually with the increase of rotational speed, and reaches to maximum ~~value~~ at 2900rpm. When rotational speed increases from 1700 to 2900rpm, the $L_{pA}$ increases by 12.40%. However, the growth slope decreases gradually with the increase of rotational speed generally, in particular, the $L_{pA}$ grows rapidly in the interval between 1700 and 2300rpm, with an average increase of 1.12dB per 100rpm, while in the range from 2300 to 2900rpm, the growth rate of $L_{pA}$ slows down, with an average increase of 0.65dB per 100rpm, which is less than that in the range from 1700 to 2300rpm. It could be explained by that with the increase of rotational speed, the pressure ~~fluctuations~~fluctuation on wall surface also ~~increase~~increases, but the increment rate of the variance of pressure ~~fluctuations~~fluctuation decreases [29~~]~~], and ~~could cause the~~ causes a slow increase of acoustic pressure around the pump ~~increases slowly~~, as a result, the growth slope of noise level decreases ~~gradually~~steadily.

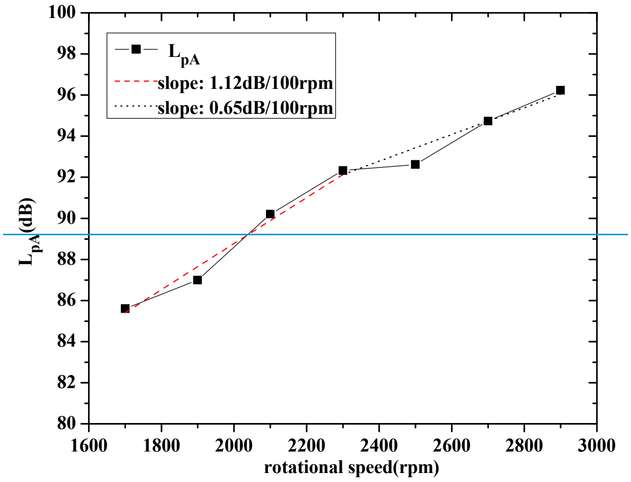


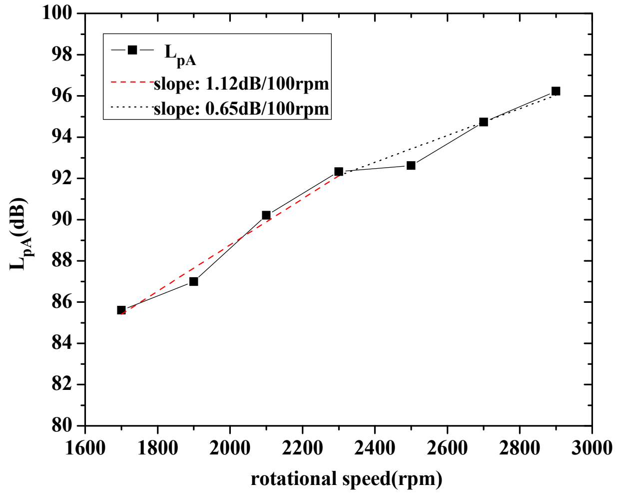


**Figure ~~7~~8.** $L_{pA}$ changing curve with rotational speed

## 4. Radiation noise characteristic under various flow rate conditions

Compared with the variable speed regulation, the throttling regulation has the advantages of easy operation and low cost. Considering the two factors mentioned, throttling regulation is widely adopted at some occasions. In this section, the throttling regulation is realized by adjusting the valve opening on outlet pipe, then five different flow rates, i.e., 37.5, 50 (~~rated~~nominal flow rate), 62.5, 75 and 86m$^3$/h (valve open fully), are studied to explore the radiation noise characteristic under various flow rate conditions when rotational speed is set as 2900rpm.

### *4.1. Directivity characteristic of radiation noise under various flow rate conditions*

By calculating the ~~TSPL~~TSPLs of 16 different points in the circumferential direction, then the directivity characteristic of radiation noise is analyzed under various flow rate conditions.

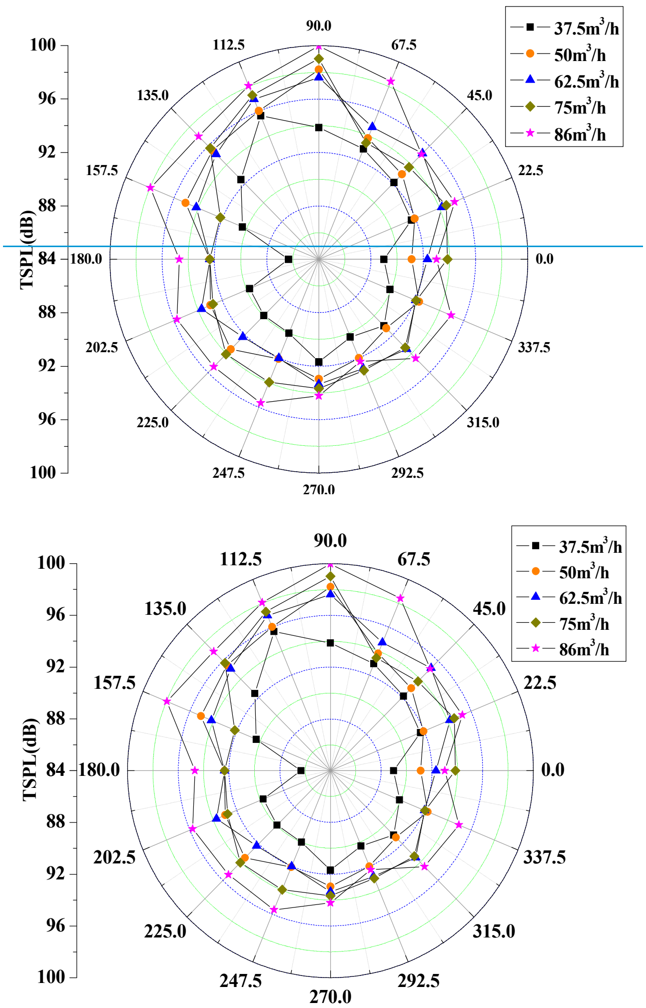


**Figure ~~8~~9.** Directivity characteristic of radiation noise under various flow rate conditions (2900rpm)

It is ~~discovered from~~ apparent in Figure ~~8~~9 that TSPL changes between 86dB and 100dB, not only the dipole characteristic, but ~~also~~ the asymmetric characteristic are presented in circumferential direction~~, which are similar to the diagram characteristic in Figure 4~~. And then the ratio of the acoustic energy in the interval from 90° to 157.5° ($\mathcal{E}_1$), as well as that in the interval from 292.5° to 0° ($\mathcal{E}_2$) to the total acoustic energy ($\mathcal{E}_t$) are compared under various flow rate conditions~~, as~~. As shown in Figure ~~9~~10, the ~~value~~values of $\mathcal{E}_1/\mathcal{E}_t$ and $\mathcal{E}_2/\mathcal{E}_t$ show the fluctuation trend in the vicinity of 0.410 and 0.166, respectively~~, which~~. And these results are closer to ~~the value of~~those under various rotational speed conditions. It also can be found that the deviation between the value of $\mathcal{E}_1/\mathcal{E}_t$ and average value (0.410) is ~~relatively~~ larger at 50$m^3$/h~~, which~~. It could be explained by that in the measurement process, the measurement results are affected by the severe disturbance of the surrounding environment, but it does not affect the conclusion that the change of flow rate also has ~~slight~~little impact on the acoustic energy distribution.

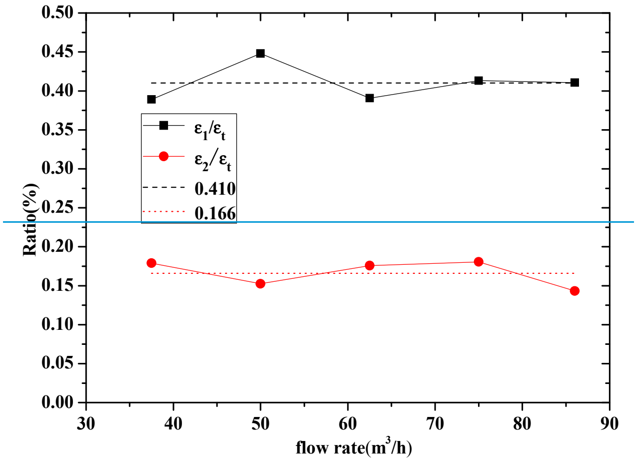


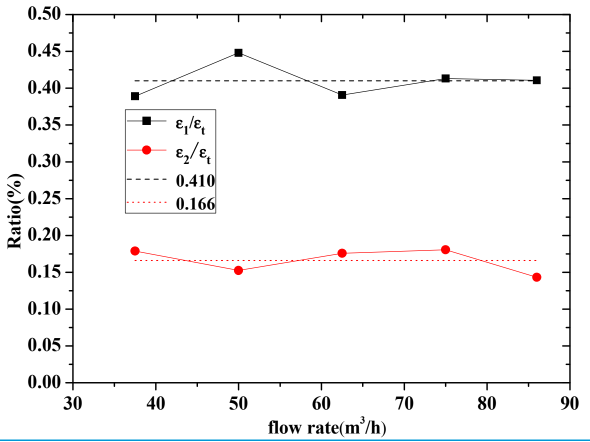


**Figure ~~9~~10.** The acoustic energy changing curves with flow rate (2900rpm)

*4.2. Changing rules of radiation noise under various flow rate conditions*

In Figure ~~10, TSPL~~11, TSPLs of P1, P5, P9, P11 and P13 are also analyzed to reveal the noise level changing rules under various flow rate conditions. It is revealed that ~~TSPL~~TSPLs of different points show the similar changing rules, specifically, the TSPL increases rapidly in small flow range from 37.5 to 50$m^3$/h, then basically levels off in the interval from 50 to 75$m^3$/h, and continues to increase when flow rate is ~~high~~higher than 75$m^3$/h. What's more, the TSPL distribution characteristic of different points under various flow rate conditions also shows that ~~P5 and P13 are~~ the ~~lowest~~ noise level ~~points, TSPL~~at P5 and P13 are lower than others, while TSPLs of P9 and P11 are higher than others, and P9 is highest noise level point, which ~~is similar to~~coincides with the distribution under various rotational speed conditions.

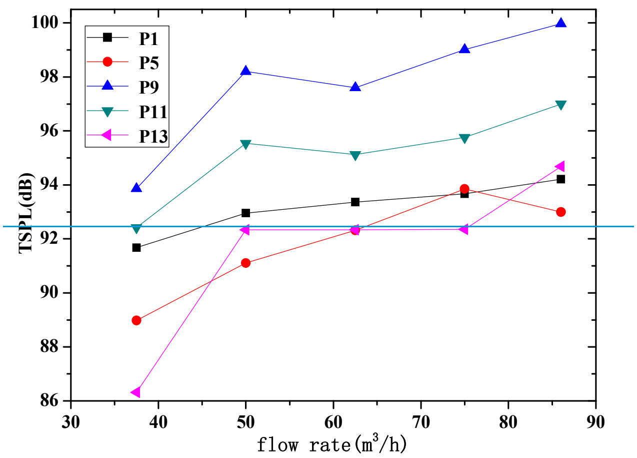


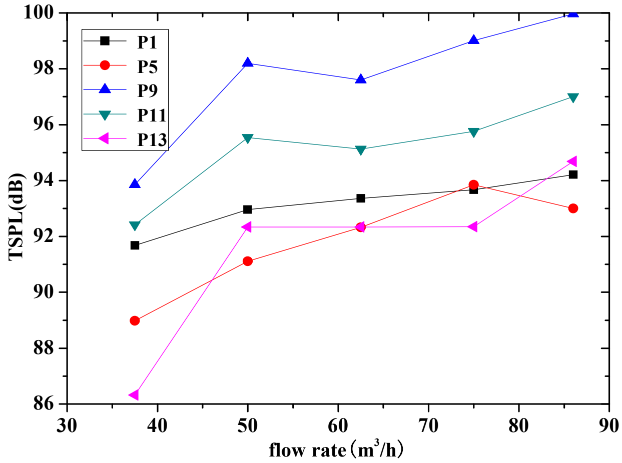


**Figure ~~10~~11.** TSPL changing curves with flow rate (2900rpm)

Furthermore, $L_{pA}$ of 16 monitoring points is also studied under various flow rate conditions. It can be found in Figure ~~11~~12 that the $L_{pA}$ ~~shows the same changing trend with the TSPL of different monitoring points that~~also increases sharply ~~firstly~~initially at small flow rate, then maintains ~~stably~~stable, and reaches to maximum value at large flow rate interval. Additionally, $L_{pA}$ changes a little with the increase of flow rate, which increases by 5.10% when flow rate grows from 37.5 to 86m$^3$/h.

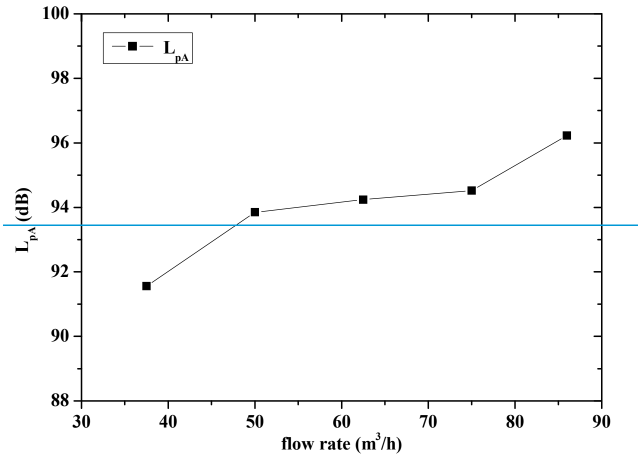


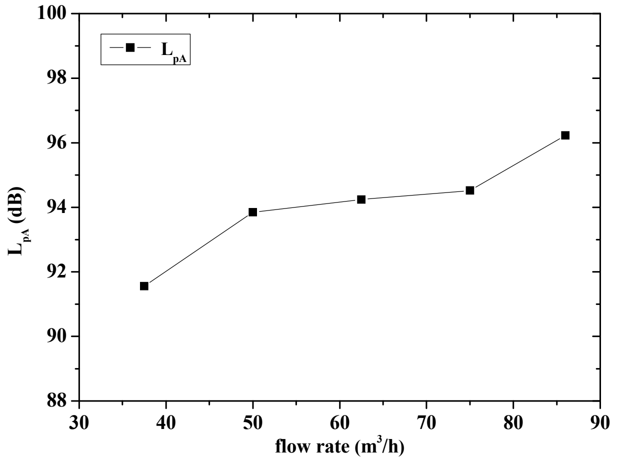


**Figure ~~11~~12.** $L_{pA}$ changing curve with flow rate (2900rpm)

To explore the reasons for the changing ~~rule~~rules of $L_{pA}$ under various flow rate conditions, the head and efficiency are calculated, respectively. The changing rules of the two parameters are shown in Figure ~~12~~13, it can be found that with the increase of flow rate, the head decreases gradually~~, in~~. In addition, the efficiency shows the tendency that increases~~ firstly~~ from 37.5 to 50m$^3$/h, and reaches to the maximum at 50m$^3$/h, then remains essentially unchanged in the range from 50 to 75m$^3$/h, which is the best efficiency range, and it keeps decreasing subsequently with the flow rate continues to grow. At low flow rate conditions, the pressure fluctuation inside the pump is low and causes low noise level~~, when~~. With the increase of flow rate~~ increases~~, the pressure ~~fluctuations~~fluctuation inside the pump ~~increase~~increases accordingly, while in the best efficiency range, i.e., in the range from 50 to 75m$^3$/h, the pressure becomes stable [~~16], which causes~~17], and leads to little change for the noise level~~ change little, but~~. However, as the flow rate continues to increase, the head and efficiency decrease ~~sharply~~dramatically, which may be caused by the occurrence of cavitation inside the pump, and ~~lead~~contribute to the dramatic increase of $L_{pA}$ when flow rate is larger than 75 m³/h.

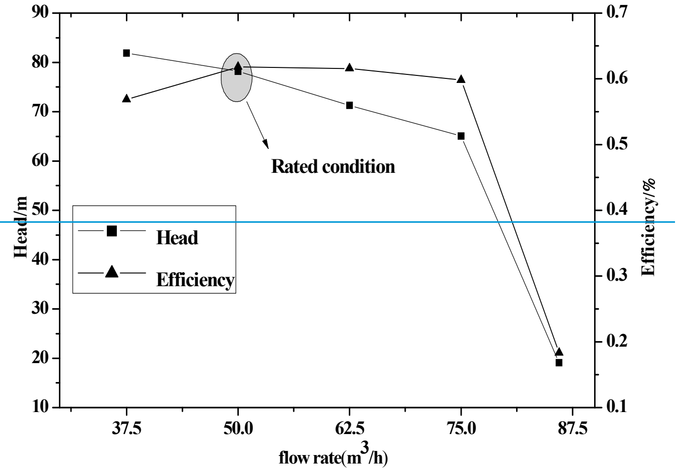


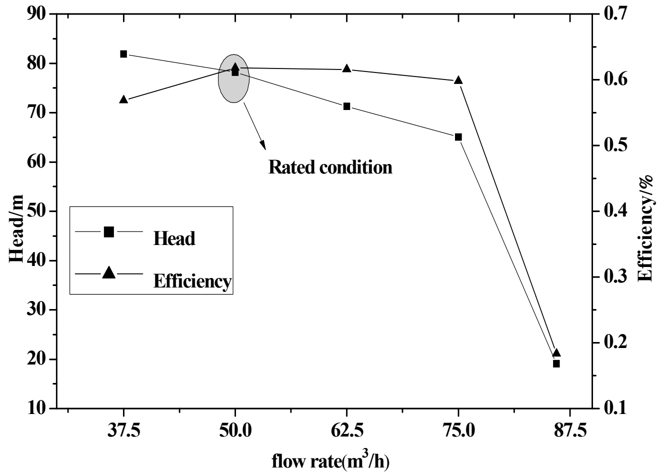


**Figure ~~12~~13.** Head and efficiency changing curve with flow rate (2900rpm)

## 5. Conclusions

In this paper, a centrifugal pump radiation noise measurement system ~~of centrifugal pump~~ is established, then the directivity distribution characteristic and overall level characteristic of radiation noise ~~on measurement surface~~ are analyzed under various working conditions. The main conclusions are drawn as follows,

a). Under various working conditions, the total sound pressure level distribution for different monitoring points ~~in circumferential direction~~ manifests the dipole characteristic, specifically, the two valley values appear at 0° (in the direction against the tongue) and 180°, and the minimum valley values are presented at the minimum rotational speed and minimum flow rate condition~~, respectively.~~. Additionally, asymmetric characteristic ~~that~~is also validated, i.e., the noise level in the direction facing the volute tongue is higher than that in the direction against the tongue~~ is also validated~~, and the monitoring point in outlet direction is the highest noise level point.

b). The change of working condition has ~~slight~~little impact on the acoustic energy distribution of different intervals, and the ratio of the acoustic energy in the direction facing the tongue ($\mathcal{E}_1$), as well as that in the direction against the tongue ($\mathcal{E}_2$) to the total acoustic energy ($\mathcal{E}_t$) ~~fluctuates~~fluctuate around 0.410 and 0.160, respectively~~, under various working conditions~~.

c). In the operation of variable speed regulation, the average A-weighted sound pressure level ($L_{pA}$) increases gradually with the increasing of rotational speed, and it increases by 12.40% when rotational speed increases from 1700 to 2900rpm, but the growth slope decreases gradually with the rise of pump rotational speed. While in the operation of throttling regulation, $L_{pA}$ shows the trend that increases firstly, then maintains stably, and continues to increase with the increase of flow rate, and it increases by 5.10% when flow rate grows from 37.5 to 86m$^3$/h.

**Acknowledgement:** This paper is supported by National Natural Science Foundation of China (~~51776111~~No.51776111), Shandong Province Natural Science Foundation (No.ZR2016EEM35), and National Development and Reform Commission Foundation (No.2013-1819)).

**Author Contributions:** Chang Guo, Dongyue Lu designed the study, conducted the experiment and collected the experimental data; Kun Wang analyzed the experimental data; Chang Guo wrote the manuscript; Ming Gao reviewed and edited the manuscript.

**Conflicts of Interest:** The authors declare no conflict of interest.

## References


1. Mao, D.X.; Hong, Z.H. Environmental Noise Control Engineering, Higher Education Press, Beijing, **2002**.
2. Shah, S.R., Jain, S.V., Patel, R.N., Lakhera, V.J. CFD for centrifugal pumps: a review of the state-of-the-art. *Procedia Eng.* **2013**, *51*, 715-720.
3. Wu, D.F., Liu, Y.S., Li, D.L., Zhao, X.F., Li, C. Effect of materials on the noise of a water hydraulic pump used in submersible. *Ocean Eng.* **2017**, *131*, 107-113.
4. Choi, J.S.; Mclaughlin, D.K.; Thompson, D.E. Experiments on the unsteady flow field and noise generation in a centrifugal pump impeller. *J.Sound Vib.* **2003**, *263*, 493-514.
5. Chu, S.; Dong, R.; Katz, J. Relationship between unsteady flow, pressure fluctuation, and noise in a centrifugal pump—part A: Use of PDV data to compute the pressure field. *J. Fluid Eng.* **1995**, *117*, 24-29.
6. Chu, S.; Dong, R.; Katz, J. Relationship between unsteady flow, pressure fluctuation, and noise in a centrifugal pump—part B: Effects of blade-tongue interactions. *J. Fluid Eng*. **1995**, *117*, 30-35.
7. Dong, R., Chu, S., Katz, J. Effect of Modification to Tongue and Impeller Geometry on Unsteady Flow, Pressure Fluctuations, and Noise in a Centrifugal Pump. *J. Turbomach.* **1997**, *119*, 506-515.

8. Parrondo, J., Pérez, J., Barrio, R., González, J. A simple acoustic model to characterize the internal low frequency sound field in centrifugal pumps. *Appl. Acoust.* **2011**, *72*, 59-64.
9. Cai, J.C., Pan, J., Andrew, G. Experimental study of the pressure fluctuation around the volute tongue of a centrifugal pump at variable rotating speed. *Fluid Mach.* **2015**, *43*, 13-16.
10. Rzentkowski, G.; Zbroja, S. Experimental characterization of centrifugal pumps as an acoustic source at the blade-passing frequency, *J. Fluid Struct.* **2000**, *14*, 529-558.
11. Wang, Q.Y. Numerical and experimental research on the flow-induced noise of centrifugal pump in the seawater pipe. M. S. thesis, Harbin Engineering University, Harbin, **2010**.
12. Si, Q.R., Yuan, S.Q., Yuan, J.P. Experimental study on the influence of impeller-tongue gap on the performance and flow-induced noise characteristics of centrifugal pumps, *J. Vib. Shock* **2016**, *35*, 164-168.
13. Yuan, S.Q., Yang, Y., Yuan, J.P., Luo, Y. Measurement system design of flow-induced noise in centrifugal pumps. *Drain. Irrig. Mach.* **2009**, 27, 10-14.
14. Liu, H.L., Wang, Y., Yuan, S.Q., Tan, M.G. Effects of impeller outlet width on the vibration and noise from centrifugal pumps induced by flow. *J. Huazhong Univ. of Sci. & Tech. (Natural Science Edition)* **2012**, *40*, 123-127.
15. Tan, M.G., Wang, Y., Liu, H.L., Wu, X.F., Wang, W. Effects of number of blades on flow induced noise vibration and noise of centrifugal pumps. *J. Drain. Irrig. Mach. Eng.* **2012**, *30*, 131-135.
16. Wang, Y., Liu, H.L., Liu, D.X., Wang, J., Wu, X.F. Effects of vane wrap angle on flow induced vibration and noise of centrifugal pumps, *T. Chin. Soc. Agric. Eng.* **2013**, *29*, 72-77.
17. Ye, X.M.; Pei, J.J.; Li, C.X.; Liu, Z. Experimental Study on Nosie Characteristics of Centrifugal Pump Based on Near-Field Acoustic Pressure Method, *Chin.J. Power Eng.* **2013**, *33*, 375-380.
18. Wang, M., Freund, J. B., Lele, S. K. Computational prediction of flow-generated sound. *Annu. Rev. Fluid Mech.* **2015**, *38*, 483-512.
19. Liu, H.L.; Dai, H.W.; Ding, J.; Tan, M.G.; Wang, Y.; Huang, H.Q. Numerical and experimental studies of hydraulic noise induced by surface dipole sources in a centrifugal pump. *J. Hydrodyn.* **2016**, *28*, 43-51.
20. Langthjem, M.A.; Olhoff, N. A numerical study of flow-induced noise in a two-dimensional centrifugal pump. Part I. Hydrodynamics. *J. Fluid Struct.* **2004**, *19*, 349-368.
21. Langthjem, M.A.; Olhoff, N. A numerical study of flow-induced noise in a two-dimensional centrifugal pump. Part II. Hydroacoustics. *J. Fluid Struct.* **2004**, *19*, 36-386.
22. Huang, J.X.; Geng, S.J.; Wu, R.; Liu, K.; Nie, C.Q.; Zhang, H.W. Comparison of noise characteristics in centrifugal pumps with different types of impellers. *Acta Acoust.* **2010**, *35*, 113-118.
23. Ma, Z.L., Chen, E.Y., Guo, Y.L., Yang, A.L. Numerical Simulation of the Influence of the Diameter at the Outlet of an Impeller on the Noise Level Induced by the Flow Inside a Centrifugal Pump. *J. Eng. Therm. Energ. Power* **2016**, *31*, 93-98.
24. Liu, H.L., Ding, J., Tan, M.G., Cui, J.B., Wang, Y. Analysis and experimental of centrifugal pump noise based on outlet width of impeller. *T. Chin. Soc. Agric. Eng.* **2013**, *29*, 66-73.

25. Gao, M.; Dong, P.X.; Lei, S.H.; Turan, A. Computational Study of the Noise Radiation ina Centrifugal Pump When Flow Rate Changes. *Energies* **2017**, *10*.
26. Dong, P.X., Gao, M., Guan, H.J., Lu, D.Y., Song, K.Q., Sun, F.Z. Numerical simulation for variation law of volute radiated noise in centrifugal pumps under variable rotating speed. *J. Vib. Shock* **2017**, *36*, 128-133.
27. Tao, J.Y., Lu, X.N., Wang, L.L Methods of measuring and evaluating noise of pumps, Chinese Quality Supervision Bureau, Beijing, China, **2013**.
28. Du, G.H., Zhu, Z.M., Gong, X.F. Fundamentals of acoustics, Nanjing University Press, Nanjing, China, **2001**.
29. Dong, P.X. Computational study on the noise radiation of a centrifugal pump based on 3-D flow field with varying working condition, M.S. thesis, Shandong University, Jinan, **2016**.